SCOPE2: OBJECT-ORIENTED PARALLEL CODE FOR MULTI-GROUP DIFFUSION/TRANSPORT CALCULATIONS IN THREE-DIMENSIONAL FINE-MESH REACTOR CORE GEOMETRY

Masahiro Tatsumi and Akio Yamamoto
Fuel Engineering and Development Department, Nuclear Fuel Industries, Ltd.
950 Ohaza Noda, Kumatori-cho, Sennan-gun, Osaka 590-0481, Japan
tatsumi@nfi.co.jp ; a-yama@nfi.co.jp

ABSTRACT

A parallel production core calculation code SCOPE2 has been developed. SCOPE2 performs multi-group diffusion/transport calculations for nuclear design in 3-D fine-mesh (i.e. pin-by-pin) geometry and runs on parallel environments such as PC clusters. The multi-group diffusion/SP3 transport equations are solved by the Red/Black iterative method within the framework of the conventional finite difference or the advanced nodal method without non-linear iterations. In this paper, the response matrix formulation of the SP3 equation in the advanced nodal method is derived followed by the derivation of an analytic solution of the flux moments in the SP3 transport equations. Numerical results in assembly and PWR core geometry showed good accuracy of the present method. SCOPE2 gave almost perfect scalability for a large problem with a PC cluster of 16 Pentium-4 processors connected with 100BASE-T network. A typical 9-group depletion calculation in the 3-D fine-mesh full-core geometry of 3 loop-type PWR was performed in 4.4 hours with 16 processors.

1. INTRODUCTION

Improvement of prediction accuracy for core characteristics is necessary from the viewpoint of reliability and cost effectiveness. Availability of affordable high-performance computing systems encourages development of highly accurate core calculation methods. The three-dimensional fine-mesh multi-group transport calculation is one of the most promising methods for advanced core analyses, however this is still challenging on average computing platforms.

Feasibility studies were successfully done through development of SCOPE[1], a proto-type parallel code based on the object-oriented multi-group transport calculation in three-dimensional fine-mesh (i.e. pin-by-pin) geometry. For the next step, SCOPE2 has been developed as a production level core calculation code for PWR. The calculation kernel was redesigned and implemented in the C++ using the expression template technique[2] and the standard template library (STL) for better performance and maintainability.

SCOPE2 solves steady-state physics in reactor core based on multi-group diffusion and/or transport theory methods in three-dimensional fine-mesh geometry. Therefore SCOPE2 can treat directly heterogeneity in each fuel assembly and spectral mismatch at an interface between different types of fuel assemblies. Neutron balance is calculated with the response matrix formulation using pin-wise cross sections corrected by the SPH method[3], then global distribution of neutron flux is obtained within the framework of an iterative method based on the Red/Black sweep. The cross-section scaling

acceleration method[4], the coarse-mesh diffusion acceleration[5] and flux extrapolation by the Chebyshev acceleration[6] are used to reduce computation time.

Features indispensable for design calculations were fully implemented such as depletion, neutron-thermal feedback, Xe-Sm transient, branching and reloading, critical boron concentration or k-eff search, RCC-bank insertion/withdrawal, and geometrical transformation between quarter and full core geometry. Depletion calculation can be performed with either a macroscopic burnup model with correction by spectral history or a microscopic burnup model by tracking explicitly 39 burnable nuclides in each mesh. Macroscopic and miscroscopic cross sections are synthesized from the pre-calculated cross section tables as a function of burnup, fuel temperature, moderator temperature, void fraction and so on. CASMO-4[7] was used for preparation of the cross section tables.

SCOPE2 runs on distributed/parallel environments including Beowulf[8] using the MPI library[9]. In parallel executions, identical converged solutions with those in serial execution are guaranteed by a fine-grained parallel algorithm. Reloading and/or branching calculations can be performed using MPI-I/O functions[10] with any numbers of processors with the restart files created in serial/parallel calculations.

In this paper, we discuss the calculation model and the parallel model in SCOPE2 that is needed for fast computation in 3-D fine-mesh geometry. Section 2 gives the response matrix formulation in the advanced nodal method and the analytic solution of the multi-group SP3 transport equation. Section 3 briefly reviews a fine-grained parallel algorithm in SCOPE2. Numerical results are given for assembly and core calculations in Section 4 followed by a discussion on parallel performance in Section 5. Finally we conclude in Section 6.

2. CALCULATION MODEL

2.1 RESPONSE MATRIX FORMULATION BASED ON THE SP3 ADVANCED NODAL METHOD

A straightforward way is adopted in SCOPE2 to accurately calculate neutronic parameters: the fine-mesh multi-group transport calculation. The fine-mesh 3-D geometry in the finite difference method is very simple to handle where no special assumptions exist; it is obvious that it gives a good answer when the mesh size is small enough. Treatment in the multi-group formulation is desirable in advanced calculation codes for applicability to systems with steep change of neutron spectrum such as a partially loaded MOX core. Furthermore, the transport theory method would be desired for reliability of solutions.

Resolution of spatial mesh is one of the most important parameter to give good calculation accuracy. It is also important in preparation of mesh-wise cross sections corrected by the SPH method because the accuracy of the correction factor depends on the level of mesh division. The more spatial mesh, the more accurate cross sections can be used. However it is not practical to divide a pin cell into 3x3 mesh or more in radial direction from the viewpoint of computing time. Then a smart method is needed to gives good accuracy within realistic computing cost. Therefore we adopted the simplified P3 (SP3) transport theory method[11] within the framework of advanced nodal methods (ANMs). An advanced method in SCOPE2 is treated by the analytic coarse mesh finite difference method originally proposed by Chao[12][13]. The formulation in Ref. 12 requires nonlinear iterations[14] to

determine coupling coefficients including k_∞. For simplicity and efficiency for parallel execution, therefore, we extended it to a response matrix formulation that does not require nonlinear iterations. Here we derive the response matrix formulation in the advanced nodal method for the SP3 transport theory.

The SP3 transport equation with isotropic scattering can be written as follows with the standard notation:

$$-D_g\nabla^2(\phi_g^0+2\phi_g^2)+\Sigma_{r,g}(\phi_g^0+2\phi_g^2)=\frac{\chi_g}{k_{eff}}\sum_{g'}\nu\Sigma_{f,g'}\phi_{g'}^0+\sum_{g'\neq g}\Sigma_{s,g'\to g}\phi_{g'}^0+2\Sigma_{r,g}\phi_g^2 \tag{1-a}$$

$$-\frac{27}{35}D_g\nabla^2\phi_g^2+\Sigma_t\phi_g^2=\frac{2}{5}\left(\Sigma_{r,g}\phi_g^0-(\frac{\chi_g}{k_{eff}}\sum_{g'}\nu\Sigma_{f,g'}\phi_{g'}^0+\sum_{g'\neq g}\Sigma_{s,g'\to g}\phi_{g'}^0)\right) \tag{1-b}$$

Some manipulations gives

$$\nabla^2\Phi_g-\left(\kappa_g^0\right)^2\Phi_g=-\frac{1}{D_g^0}S_g^0 \tag{2-a}$$

$$\nabla^2\phi_g-\left(\kappa_g^2\right)^2\phi_g=-\frac{1}{D_g^2}S_g^2 \quad , \tag{2-b}$$

where

$$\begin{aligned}
&\Phi_g=\phi_g^0+2\phi_g^2\\
&D_g^0=D_g\ ,\ \ D_g^2=\frac{27}{35}D_g\ ,\quad \kappa_g^0=\sqrt{\frac{\Sigma_{r,g}}{D_g^0}}\ ,\ \kappa_g^2=\sqrt{\frac{\Sigma_{t,g}}{D_g^2}}\\
&S_g^0=\frac{\chi_g}{k_{eff}}\sum_{g'}\nu\Sigma_{f,g'}\phi_{g'}^0+\sum_{g'\neq g}\Sigma_{s,g'\to g}\phi_{g'}^0+2\Sigma_{r,g}\phi_g^2\\
&S_g^2=\frac{2}{5}\left(\Sigma_{r,g}\phi_g^0-(\frac{\chi_g}{k_{eff}}\sum_{g'}\nu\Sigma_{f,g'}\phi_{g'}^0+\sum_{g'\neq g}\Sigma_{s,g'\to g}\phi_{g'}^0)\right)
\end{aligned} \tag{3}$$

Eqs. (2-a) and (2-b) has the same form, thus hereafter we focus on the equation for the fundamental mode. For the x-axis, Eq. (2-a) can be written as,

$$\frac{d^2\Phi_g}{dx^2}-\left(\kappa_g^0\right)^2\Phi_g=-\frac{1}{D_g^0}\left(S_g^0-\frac{(J_{y+}^0-J_{y-}^0)}{h_y}-\frac{(J_{z+}^0-J_{z-}^0)}{h_z}\right) \tag{4}$$

where

J_{d+}^0 = net current at the surface of right side (+) in the direction of d,

h_d = mesh width in direction of d.

In Eq. (4), we introduced an assumption on flat-source distribution inside a mesh. In fine-mesh systems where the mesh size is ~ 1cm, it may be a good assumption. If not, the source distribution can be easily considered by introducing a polynomial function. Determination for treatment of source distribution would be determined through further study. Then the source is corrected by transverse leakage calculated within inner-iterations. Therefore the present method does not require additional non-linear iteration to update coefficients in finite difference formulation for partial currents.

In solving Eq. (4), we have five unknowns as two coefficients in solution of flux distribution, two out-going currents at the boundaries, and a node-average flux. With two constraints for net currents at the node boundaries, two for surface fluxes, and one for neutron balance in a node, we can obtain an analytic solution,

$$J^{0+}_{x+,g} = \mu^0_g J^{0-}_{x+,g} + \eta^0_g \Phi_g + \xi^0_g S^{0,x}_g \tag{5}$$

where

$$\mu^0_g = \frac{\left(1-\frac{4}{h_x}D^{0*}_g\right)}{\left(1+\frac{4}{h_x}D^{0*}_g\right)}\ ,\ \eta^0_g = \frac{\frac{2}{h_x}D^{0*}_g\gamma^0_g}{\left(1+\frac{4}{h_x}D^{0*}_g\right)}\ ,\xi^0_g = \frac{-1+\exp(2h_x\kappa^0_g)-2\exp(h_x\kappa^0_g)h_x\kappa^0_g}{\left(-1+\exp(h_x\kappa^0_g)\right)^2\left(1+\frac{4}{h_x}D^{0*}_g\right)\kappa^0_g}$$

$$D^{0*}_g = D^0_g * \frac{(1+\exp(h_x\kappa^0_g))h_x\kappa^0_g}{2(-1+\exp(h_x\kappa^0_g))} \tag{6}$$

$$\gamma^0_g = \frac{2\exp(h_x\kappa^0_g)h_x\kappa^0_g}{-1+\exp(2h_x\kappa^0_g)}$$

$$S^{0,x}_g = S^0_g - \frac{(J^0_{y+}-J^0_{y-})}{h_y} - \frac{(J^0_{z+}-J^0_{z-})}{h_z}$$

For other directions and the second-order moment, analytic solutions can be obtained in the same manner. The coefficients μ, η and ξ are recalculated when cross sections are updated in thermal and/or boron feedback. This is done once in several outer iterations. Therefore calculation of out-going currents is very simple and quick by simple arithmetic operation with in-coming currents from adjacent mesh and mesh-average flux calculated by the direct inversion method described in the next subsection.

2.2 MOMENT CALCULATION BY DIRECT MATRIX INVERSION

In solving Eqs. (2-a) and (2-b), iterative method on the flux moments can be used[15]. However the flux moments ϕ^0_g and ϕ^2_g can be solved analytically with Eqs. (1-a) and (1-b) by direct matrix inversion. Here we derive the analytic solution of the flux moments.

We have the SP3 transport equation in the ANM as follows:

$$
\begin{aligned}
(V\Sigma_{r,g} + (2h_y h_z \eta_x^0 + 2h_x h_z \eta_y^0 + 2h_x h_y \eta_z^0))\Phi_g = \; & VS_g^0 \\
& -h_y h_z((\mu_x^0 - 1)(J_{x+}^{0-} + J_{x-}^{0-})) \\
& -h_x h_z((\mu_y^0 - 1)(J_{y+}^{0-} + J_{y-}^{0-})) \\
& -h_x h_y((\mu_z^0 - 1)(J_{z+}^{0-} + J_{z-}^{0-})) \\
& -2h_y h_z \xi_x^0 S_g^{0,x} - 2h_x h_z \xi_y^0 S_g^{0,y} - 2h_x h_y \xi_z^0 S_g^{0,z}
\end{aligned}
\tag{7-a}
$$

$$
\begin{aligned}
(V\Sigma_{t,g} + (2h_y h_z \eta_x^2 + 2h_x h_z \eta_y^2 + 2h_x h_y \eta_z^2))\phi_g^2 = \; & VS_g^2 \\
& -h_y h_z((\mu_x^2 - 1)(J_{x+}^{2-} + J_{x-}^{2-})) \\
& -h_x h_z((\mu_y^2 - 1)(J_{y+}^{2-} + J_{y-}^{2-})) \\
& -h_x h_y((\mu_z^2 - 1)(J_{z+}^{2-} + J_{z-}^{2-})) \\
& -2h_y h_z \xi_x^2 S_g^{2,x} - 2h_z h_z \xi_y^2 S_g^{2,y} - 2h_x h_y \xi_z^2 S_g^{2,z}
\end{aligned}
\tag{7-b}
$$

where $S_g^{m,d}$ is the effective neutron source along an axis $d \in \{x, y, z\}$ subtracted the transverse leakage and V is a volume of the mesh. For example, for x axis,

$$
S_g^{0,x} = S_g^0 - \frac{(J_{y+}^0 - J_{y-}^0)}{h_y} - \frac{(J_{z+}^0 - J_{z-}^0)}{h_z} \equiv S_g^0 - R_g^{0,x} \tag{8}
$$

Eqs. (7-a) and (7-b) can be simplified as

$$
\begin{aligned}
(V\Sigma_{r,g} + 2\eta^0)(\phi_g^0 + 2\phi_g^2) = \; & VS_g^0 - H_x \mathrm{M}_x^0 - H_y \mathrm{M}_y^0 - H_z \mathrm{M}_z^0 \\
& - 2H_x \xi_x^0 S_g^{0,x} - 2H_y \xi_y^0 S_g^{0,y} - 2H_z \xi_z^0 S_g^{0,z}
\end{aligned}
\tag{9-a}
$$

$$
\begin{aligned}
(V\Sigma_{t,g} + 2\eta^2)\phi_g^2 = \; & VS_g^2 - H_x \mathrm{M}_x^2 - H_y \mathrm{M}_y^2 - H_z \mathrm{M}_z^2 \\
& - 2H_x \xi_x^2 S_g^{2,x} - 2H_y \xi_y^2 S_g^{2,y} - 2H_{zy} \xi_z^2 S_g^{2,z}
\end{aligned}
\tag{9-b}
$$

where

$$
\begin{aligned}
& \eta^m = h_y h_z \eta_x^m + h_x h_z \eta_y^m + h_x h_y \eta_z^m \\
& H_x = h_y h_z \;,\; H_y = h_x h_z \;,\; H_z = h_x h_y \\
& \mathrm{M}_d^m = (\mu_d^m - 1)(J_{d+}^{m-} + J_{d-}^{m-}) \quad (m = 0,2 \text{ and } d = x, y, z)
\end{aligned}
\tag{10}
$$

With the neutron source defined as

$$
S_g = \frac{\chi_g}{k_{eff}} \sum_{g'} \nu\Sigma_{f,g'} \phi_{g'}^0 + \sum_{g' \neq g} \Sigma_{s,g' \to g} \phi_{g'}^0 \quad , \tag{10}
$$

the effective neutron source for each moment can be written as follows:

$$S_g^0 = S_g + 2\Sigma_{r,g}\phi_g^2$$
$$S_g^2 = \frac{2}{5}\left(\Sigma_{r,g}\phi_g^0 - S_g\right) \tag{11}$$

Omitting the index g, then the SP3 transport equation based on the advance nodal method can be written in the matrix form as

$$\begin{pmatrix} 2\eta^0 + V\Sigma_r & 4(\eta^0 + \xi^0\Sigma_r) \\ -\frac{2}{5}(V - 2\xi^2)\Sigma_r & 2\eta^2 + V\Sigma_t \end{pmatrix}\begin{pmatrix}\phi^0 \\ \phi^2\end{pmatrix} = \begin{pmatrix} S(V - 2\xi^0) - \mu^0 + 2X^0 \\ -\frac{2}{5}S(V - 2\xi^2) - \mu^2 + 2X^2 \end{pmatrix} \tag{12}$$

where

$$\mu^m \equiv H_x \mathrm{M}_x^m + H_y \mathrm{M}_y^m + H_z \mathrm{M}_z^m$$
$$\xi^m \equiv H_x \xi_x^m + H_y \xi_y^m + H_z \xi_z^m \tag{13}$$
$$X^m \equiv H_x \xi_x^m R^{m,x} + H_y \xi_y^m R^{m,y} + H_z \xi_z^m R^{m,z} \quad , \quad (m = 0, 2)$$

Solving Eq. (12), we can obtain a pair of analytic solutions for flux moment:

$$\phi^0 = \frac{S(V - 2\xi^0) - \mu^0 + 2X^0 - 4(\eta^0 + \xi^0\Sigma_r)\phi^2}{2\eta^0 + V\Sigma_r} \tag{14-a}$$

$$\phi^2 = -\frac{\frac{2}{5}\left\{-S(V - 2\xi^0) + \mu^0 - 2X^0\right\}(V - 2\xi^2)\Sigma_r + \left\{\frac{2}{5}S(V - 2\xi^2) + \mu^2 - 2X^2\right\}(2\eta^0 + V\Sigma_r)}{\frac{8}{5}(V - 2\xi^2)\Sigma_r(\eta^0 + \xi^0\Sigma_r) + (2\eta^0 + V\Sigma_r)(2\eta^2 + V\Sigma_t)} \tag{14-b}$$

Note that the solution in the conventional finite difference method is obtain under the conditions,

$$\xi^m \to 0, \quad X^m \to 0$$

as

$$\phi^0 = \frac{SV - \mu^0 - 4\eta^0\phi^2}{2\eta^0 + V\Sigma_r} \tag{15-a}$$

$$\phi^2 = -\frac{4VS\eta^0 + 10\eta^0\mu^2 + V\Sigma_r(2\mu^0 + 5\mu^2)}{5V\Sigma_r\left(2\eta^2 + V\Sigma_t\right) + 2\eta^0\left(10\eta^2 + 4V\Sigma_r + 5V\Sigma_t\right)} \quad . \tag{15-b}$$

With the flux moments and in-coming currents at the surface of the mesh, we can obtain the out-going currents using the response described by Eq. (5).

3. IMPLEMENTATION

A three-dimensional fine-mesh calculation system consists of *Block* objects, typically a set of 10x10x1 fine meshes. In the case of a 17x17 fuel assembly for PWR, a radial cross section of a fuel assembly can be build with 4 *Blocks*. The *RBlock* class for reflector region maintains cross sections, out-going partial currents, neutron fluxes and scattering sources, and other parameters for feedback calculation in each mesh. The *FBlock* class derived from *RBlock* maintains also fission source and the parameters for burnup calculations. Arbitrary calculation theory can be assigned to each fine mesh in both types of *Block* independently. The diffusion theory or the SP3 transport theory methods within the framework of the conventional finite difference or the advanced nodal method are currently implemented in SCOPE2.

A calculation system is constructed as a set of *Block* objects in 3-D geometry, which is maintained in a *Container* object. In parallel execution, a *Container* object is decomposed into arbitrary 2-D shapes. No division is performed on z-axis for better performance in feedback calculations.

The fine mesh is categorized into two types: red and black. In a red mesh, for example, a response calculation can be done with in-coming neutron partial currents from six adjacent black meshes. With even number of mesh division in radial directions, each *Block* can perform the response calculation independently if the *Block* is not on the processor boundary. This division scheme is effective for good parallel efficiency since a latency-hidden algorithm can be easily implemented by (1) initiating non-blocking communications for updating partial currents on processor boundaries, (2) performing response calculations for Blocks not on the processor boundaries, (3) performing response calculation for the Blocks on the boundary. Normally communications would be completed by the time the response calculations finish.

Coarse-mesh and coarse-group systems for diffusion acceleration can be treated within the same framework of that in the fine-mesh system, i.e. the *Container* class. Therefore those objects can be easily initialized from the fine-mesh *Container* object in the nature of object-oriented approach. In the coarse-mesh system, discontinuity factors at the *Block* surfaces are calculated so that the neutron balance in the fine-mesh system can be preserved in the coarse-mesh system. The coarse-mesh systems are also decomposed in parallel execution and a fine-grained parallel model is adopted also in this model. The cost for communication become relatively large compared to the fine-mesh system, it is a key point to determine how often the coarse-mesh calculation is performed. Currently a coarse-mesh calculation is performed every 3 outer iterations.

4. NUMERICAL RESULTS

4.1 SINGLE AND 2X2 ASSEMBLY GEOMETRY

To demonstrate accuracy of the SCOPE2 model, here we start from simple calculation in 2-D single assembly geometry. A set of depletion calculations by the SP3 advance nodal method was performed in 9-group for a 4.1wt% ^{235}U-enriched 6wt% Gd-bearing fuel assembly. In SCOPE2 calculations, the predictor/corrector method was used in the macroscopic burnup model. As shown in Fig. 1, the

burnup characteristics on k_∞ well agreed between SCPOE2 and CASMO-4 within the error of 0.06%Δk. The maximum and R.M.S. errors of pin power were at 45GWd/t was 0.60% and 0.23%, respectively as shown in Fig. 2. It is notable that effects on pin-cell homogenization were properly taken into account with the SPH correction method.

The next example is 2x2 assembly geometry of 4.1wt% and 2.0wt% enriched UO_2 fuel assemblies. This is a demonstration of proper treatment of spectrum mismatch at the interface of the assemblies with 9-group energy structure. The burnup characteristic on k_∞ of the system was well predicted by SCOPE2 within the error of 0.1%Δk. The error on pin power distribution in the central zone at 30GWd/t given in Fig. 3 shows good agreement of SCOPE2 results with CASMO-4. We found the present calculation model is able to give the accuracy of ~1% on pin power distribution while the finite difference diffusion method gives that of ~1.3%.

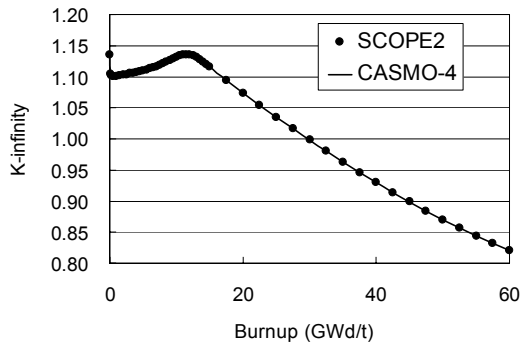

Figure 1. Reactivity change in single assemb ly geometry predicted by SCOPE2 agreed with the results by CASMO-4 in hetero-geneous model used in preparation of cross section library for SCOPE2.

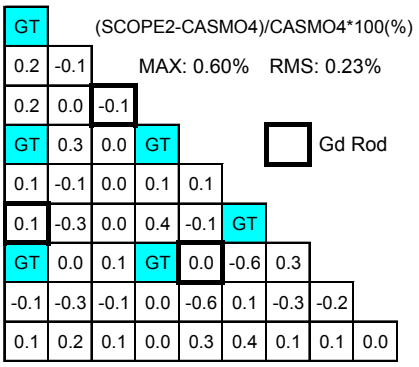

Figure 2. Error of predicted power distribution by SCOPE2 in 4.1wt% ^{235}U-enriched 6wt% Gd fuel assembly at 45GWd/t.

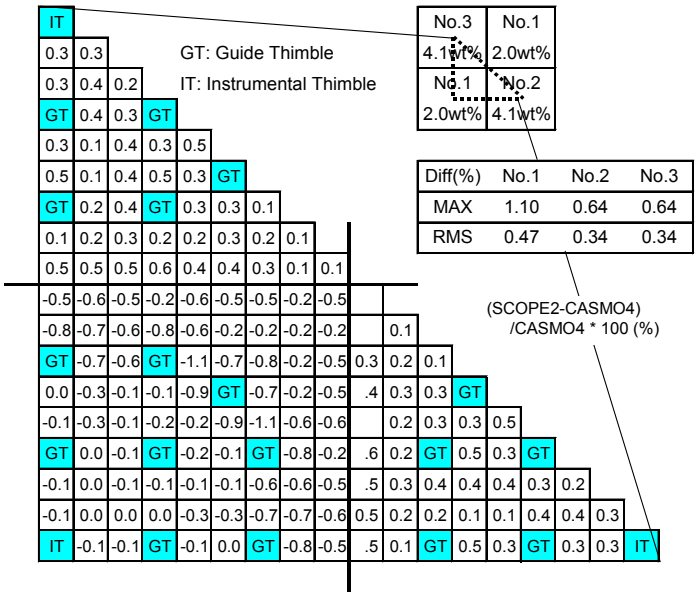

Figure 3. Pin power distribution predicted by SCOPE2 agreed well with that by CASMO-4 in the central zone of 2x2 assembly geometry of 2.0wt% and 4.1wt% UO_2 fuel assemblies.

4.3 PWR CORE GEOMETRY

For a more realistic example, we performed a tracking calculation of the first cycle of a commercial 3 loop-type PWR core. The core consists of 2.0wt%, 3.5wt% and 4.1wt% UO_2 fuel assemblies with variety types of burnable poison rod clusters. Therefore it is suitable to examine the calculation model of SCOPE2 in such a heterogeneous configuration. A core calculation was performed in 3-D full-core geometry with 340x340x26 meshes by the SP3-ANM in 9 groups.
The power distribution predicted by SCOPE2 agreed well with the measurement. Figure 4 shows the prediction error on assembly-wise power distribution at the end of cycle.

	H	G	F	E	D	C	B	A
8	0.3	0.3	0.3	0.3	-0.1	-0.1	0.1	0.0
9	0.1	0.1	0.2	0.2	-0.1	0.0	0.0	0.0
10	0.2	0.2	0.3	0.3	0.3	0.4	0.3	
11	0.1	0.1	0.1	0.1	-0.1	-0.2	-0.4	
12	-0.1	0.0	0.2	0.0	-0.4	-0.7		
13	-0.2	-0.1	0.1	-0.2	-0.8			
14	-0.2	-0.2	0.0	-0.3				
15	-0.3	-0.3						

R.M.S. : 0.26%
MAX : -0.78%

(Calc. - Meas.) / Meas. * 100 (%)

Figure 4 Prediction errors on assembly-wise power distribution at the end of cycle of a commercial 3-loop type PWR core.

5. PARALLEL PERFORMANCE

We have measured the parallel performance by SCOPE2 on a Beowulf-type PC cluster of Pentium-4 2.0GHz.

The first example is a 1/4-core system of 3 loop-type PWR with fine meshes of 170x170x18. A set of depletion calculations within the macroscopic burnup model with 2 burnup points was performed by the SP3 method using the predictor/corrector method for each processor configuration. The speed-up curve shows fairly good parallel efficiency. However the efficiency become worse with large number of processor. This is mainly because the lack of enough computing loads for a processor in the 1-group coarse-mesh diffusion acceleration with meshes of 17x17x18.

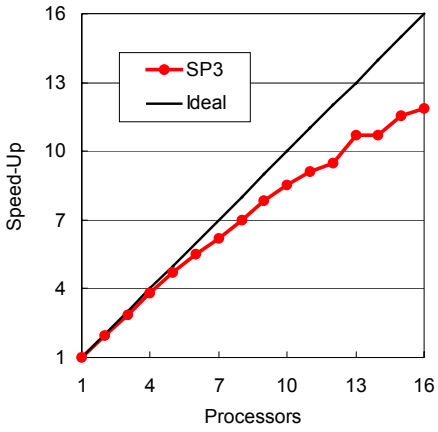

Figure 5. Speed-up curve for 3-D 1/4 co re of PWR (170x170x18 meshes)

The next example is more realistic one: a full-core geometry of 3 loop-type PWR with fine meshes of 340x340x26.
A set of depletion calculation with 12 burnup points was performed by the SP3-ANM using predictor/corrector method in macroscopic burnup model. Time profiles in computation with 6, 12, and 16 processors are listed in Table I. With 16 processors, 4.4 hours are needed for SP3-ANM calculations while 3.5 hours for the finite difference diffusion theory method.

Table I. Execution time profile in 3-D full core geometry of PWR (unit: second)

	6 Procs.	12 Procs.	16 Procs.
Initialization	21 (0.1%)	11 (0.1%)	8 (0.1%)
Fine Mesh Sweep	19584 (48.2%)	9709 (47.5%)	7391 (47.2%)
Coarse-Mesh 1-Group Diffusion Acceleration	2783 (6.8%)	1475 (7.2%)	1158 (7.4%)
Summary Edit	854 (2.1%)	570 (2.8%)	513 (3.3%)
Feedback Calc. Including XS update	16744 (41.2%)	8350 (40.8%)	6312 (40.3%)
Burnup Calc.	656 (1.6%)	342 (1.7%)	253 (1.6%)
Total	40641	20456	15648

(fraction of the item in percent)

We could not measure the computing time for serial execution because the total memory required for this calculation was ~ 4.5G bytes. Therefore a relative speed-up curve was estimated from the result with 6-processor configuration as shown in Fig. 5. The fine-mesh sweep and feedback calculations are perfectly scalable because time needed for inter-processor communication can be neglected and no communications are needed, respectively. The coarse-mesh 1-group diffusion acceleration now gives good scalability with enough computing load for each processor. Total speed-up is almost scalable since the coarse-mesh acceleration accounts for less than 10% of total computing time. The larger a problem becomes, the less time is needed for coarse-mesh diffusion acceleration. Therefore SCOPE2 gives very good scalability for large-scale problems.

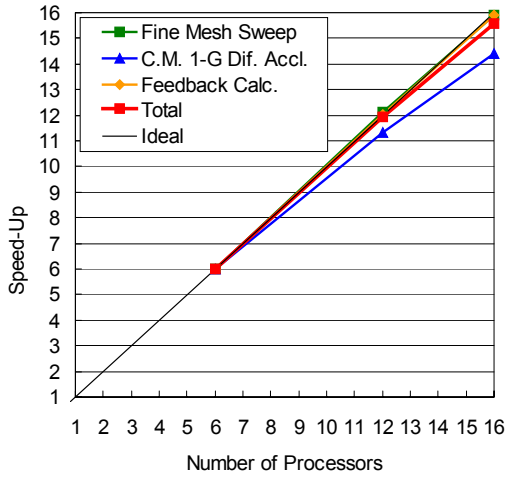

Figure 5. Speed-up curve in 3-D full-core geometry of PWR (340x340x26 meshes)

6. CONCLUSIONS

A production core calculation code SCOPE2 has been implemented by an object-oriented approach. SCOPE2 performs multi-group diffusion/transport calculations in 3-D fine-mesh pin-by-pin geometry on distributed/parallel computing environments such as PC clusters. A response matrix formulation in the advanced nodal method was derived for efficient parallel computing. Numerical results showed good accuracy of the present model in comparisons with CASMO-4 and measurement. With very good scalability on parallel environments, SCOPE2 gave good accuracy and performance for advanced reactor core analyses. Further study will be expected for verifications through tracking calculations for commercial PWR operations.

ACKNOWLEDGEMENTS

The authors would like to thank Mr. H. Hashimoto and Mr. Y. Hirai of Japan Research Institute, Ltd. for their support in implementing SCOPE2.

REFERENCES

1. M. Tatsumi and A. Yamamoto, "Object-Oriented Three-Dimensional Fine-Mesh Transport Calculation on Parallel/Distributed Environments for Advanced Reactor Core Analyses," *Nucl. Sci. Eng.*, **141**, pp 1-28 (2002).
2. T. L. Veldhuizen, "Arrays in Blitz++," *Proc. 2nd Int. Symp. Conputing in Object-Oriented Parallel Environments (ISCOPE98), Santa Fe, New Mexico, December 1998*, pp. 223-230 (1998).
3. A. Hébert, "A consistent Technique for the Pin-by-Pin Homogenization of a Pressurized Water Reactor Assembly," *Nucl. Sci. Eng.*, **113**, pp 227-238 (1993).
4. A. Yamamoto, "Acceleration of Response Matrix Method by Cross Section Scaling," *submitted to PHYSOR2002* (2002).
5. J. M. Aragonés and Carol Ahnert, "A Linear Discontinuous Finite Difference Formulation for Synthetic Coarse-Mesh Few-Group Diffusion Calculations," *Nucl. Sci. Eng*., **94**, pp. 309-322 (1986).
6. D. R. Ferguson and K. L. Derstine, "Optimized Iteration Strategies and Data Management Consideration for Fast Reactor Finite Difference Diffusion Theory Codes," *Nucl. Sci. Eng*., **64**, pp. 593-604 (1977).
7. M. Edenius, B. H. Forssen and C. Gragg, "The Physics Model of CASMO-4," *Proc. Int. Topl. Mtg. Advances in Mathematics, Computations, and Reactor Physics*, Pittsburgh, Pennsylvania, April 28-May 2, 1991, Vol. 2, p. 10.1 1-1 (1991).
8. T. Sterling, J. Salmon, D. J. Becker and D. F. Savarese, *How to build a Beowulf, A Guide to the Implementation and Application of PC Clusters*, MIT Press, Cambridge, Massachusetts (1999).
9. W. Gropp, E. Lusk and A Skejellum, *Using MPI: Portable Parallel Programming with the Message-Passing Interface*, MIT Press, Cambridge, Massachusetts (1994).
10. W. Gropp, E. Lusk and AR. Thakur, *Using MPI-2: Advanced Features of the Message-Passing Interface*, MIT Press, Cambridge, Massachusetts (1994).
11. E. M. Gelbard, "Application of Spherical Harmonics Method to Reactor Problems," WAPD-BT-20 (Sep. 1960).
12. Y. A. Chao, "A Theoretical Analysis of the Coarse Mesh Finite Difference Representation In Advanced Nodal Methods," *Proc. Int. Conf. Mathematical and Computation, Reactor Physics and Environmental Analysis in Nuclear Applications (M&C'99),* Madrid, Spain, September 1999, Vol. 1, pp. 117-126 (1999).
13. Y. A. Chao, "Coarse Mesh Finite Difference Methods and Applications*," Proc. Int. Topl. Mtg. Advances in Reactor Physics and Mathematics and Computation in the Next Millennium (PHYSOR2000),* Pittsburgh, Pennsylvania, May 7-12, IX.D-2 (2000) (CD-ROM).
14. K. S. Smith, "Nodal Method Storage Reduction by Nonlinear Iteration," *Trans. Am. Nucl. Soc.*, **44**, pp. 265-266 (1983).
15. E. W. Larsen, J. E. Morel and J. M. McGhee, "Asymptotic Derivation of the Multigroup P1 and Simplified PN Equations with Anisotropic Scattering," *Nucl. Sci. Eng.*, **123**, pp 328-342 (1996).